ELSEVIER

Biophysical Chemistry 53 (1994) 77–84

Biophysical Chemistry

Structure of dodecyl sulfate–protein complexes at subsaturating concentrations of free detergent

Konrad Ibel [a,*], Roland P. May [a], Maria Sandberg [b], Erik Mascher [b], Eva Greijer [c], Per Lundahl [c]

[a] *Institut Max von Laue-Paul Langevin, B.P. 156, F-38042-Grenoble, France*
[b] *Kabi Pharmacia, Lindhagensgatan 133, S-11287 Stockholm, Sweden*
[c] *Department of Biochemistry, Biomedical Center, Uppsala University, Box 576, S-75123 Uppsala, Sweden*

Received 20 September 1993; revised 20 November 1993; accepted 10 December 1993

Abstract

Earlier neutron small-angle scattering experiments had revealed the low resolution structure of the complex between sodium dodecyl sulfate (SDS) and the single polypeptide (452 amino acid residues) of a water-soluble enzyme. The saturated complex consists of three globular micelles (•-✹-•) which are connected by short flexible polypeptide segments. New experiments, described here, were performed at subsaturating concentrations of free SDS in equilibrium with the complex. The data show a decrease in stoichiometry from one bound dodecyl sulfate (DS) anion per two amino acid residues near the critical micelle concentration (CMC) to one per four residues at half the CMC. At 0.3 CMC, a two-micelle complex (✹-•) is formed by the recombination of the small amino-terminal micelle with the middle one; and the center-to-center distance between the carboxyl-terminal micelle and the middle one decreases from 7.5 to 6.2 nm. These structural data allow us to better understand earlier results obtained with high-performance agarose gel chromatography of the same SDS–protein complexes.

Keywords: SDS–protein complex; Neutron scattering; Critical micelle concentration; SDS binding; Protein-decorated micelle

1. Introduction

Earlier investigations of sodium dodecyl sulfate (SDS)–protein complexes have resulted in a number of partly incompatible structural models. The most prominent amongst these are the 'rod-like particle model' [1]; the 'necklace model', which is based mainly on the observation that SDS–protein complexes migrate in free-boundary electrophoresis with nearly the same velocity as do protein-free SDS micelles [2,3]; the 'random-coil-α-helix model' which explains the changes of the circular dichroism of proteins upon binding of SDS [4]; and the 'flexible-helix model' [5], which predicts that the hydrophilic segments of the polypeptide are wound around a flexible cylindrical micelle formed by the detergent molecules. The main interactions proposed to stabilize the last structure are the clustering of the dodecyl chains into a hydrophobic core and hydrogen-bonding of two sulfate groups each to the peptide NH-groups of consecutive quadruplets of amino acid residues [5].

We used N-5'-phosphoribosyl anthranilate (PRA) isomerase: indole-3-glycerol-phosphate (IGP) synthase from *Escherichia coli* [6] as a model protein for the study of the shape and the internal structure of SDS–protein complexes [7]. This protein contains 452

* Corresponding author.

SSDI 0301-4622(94)00078-X

amino acids in a single polypeptide chain without any disulfide bond. The polypeptide chain is organised in two domains of similar folding, that of an eight-fold parallel β-barrel with α-helices on the outside connecting the β-strands.

SDS denaturation of the native protein leads to the formation of three protein-binding SDS micelles: the carboxyl-terminal micelle, C; the middle micelle, M; and the amino-terminal micelle, N. These three independent and, on the average globular micelles, are connected by highly flexible linkages. Thus, the structure turned out to be similar to that proposed for dilute aqueous solutions of poly(oxyethylene)–SDS complexes [8] and to the 'necklace' model [2,3]. The main difference compared to the latter model is that the SDS in the complex forms a few large micelles in close association with nearly the entire polypeptide.

The aim of the present experiments was the observation of the mutual disposition of the three protein-decorated micelles at subsaturating concentrations of free SDS (in equilibrium with bound DS) well below the CMC. Data from agarose gel chromatography in the presence of SDS [9] indicated that the formation of the SDS–PRAI:IGPS complex is accompanied by elution volume changes within two steps, with an intermediate plateau at a free SDS concentration of 0.3 to 0.4 CMC (0.6–0.8 mM). We expected that the experiments could contribute to our understanding of the structural basis of this observation.

Our previous neutron scattering data [7] clearly answered the question of the relative distributions, within each micelle, of the hydrophobic phase which consists of the dodecyl chains (and, probably, individual hydrophobic amino acid side chains and entire hydrophobic stretches of the polypeptide chain) which are contained in the micellar cores; and the surrounding hydrophilic phase, which consists of the mostly hydrophilic segments of the polypeptide chain and the sulfate groups of the SDS molecules, similar to the 'flexible-helix' model [5]. We designated our model as the 'protein-decorated micelle structure'.

In the case of saturated complexes in solutions prepared with heavy water, the intensity of neutrons diffracted by the dodecyl chains is about ten times larger than that diffracted by the protein moiety. Neutron scattering is therefore especially well suited for the determination of the mutual disposition of the three protein-decorated micelles. Sufficiently accurate data can be obtained *without* deuteration which was necessary for the previous determination of the internal structure.

As before, the contrast variation with mixtures of ^2H_2O and ^1H_2O could be used for the determination of the number of bound DS molecules.

2. Materials and methods

2.1. Enzyme preparation

The PRA isomerase:IGP synthase was purified by standard procedures. The protein samples were equilibrated with 1.6, 1.4, 1.2, 1.0, 0.8, and 0.6 mM SDS in 0.05 M sodium phosphate, pH 6.9, 1 mM EDTA, 0.2 mM DTE, 3 mM NaN_3 by gel filtration on a 1.4×51 cm gel bed of Sephacryl S-300 HR (cf. ref. [7]) equilibrated with at least five column volumes of buffer containing SDS after each change in SDS concentration. The protein solution (800 mm^3, 11 mg/cm^3) was supplemented with an aliquot of 500 mM SDS that was estimated to give the same free SDS concentration as in the eluent, and was applied at 0.1 cm^3/min. After sample application, the flow rate was increased to 0.3 cm^3/min. For contrast variation, half of the samples were dialyzed against standard buffer (with SDS) containing 95% ^2H_2O. Intermediate concentrations of ^2H_2O were prepared by appropriate mixing of stock solutions contained in either 95% ^2H_2O or ^1H_2O. This was performed 24 h before the measurements to allow proton–deuteron exchange to reach equilibrium.

2.2. SDS binding and gel filtration

The binding was determined by gel filtration in the presence of ^{35}S-SDS on a 21-ml column of Sephacryl S-300 HR (Pharmacia LKB Biotechnology, Uppsala, Sweden). For direct measurements of ^{35}S-SDS, the column was connected to a flow scintillation detection system (FloOne/Beta, Radiomatic, Tampa, FL, USA). The column flow rate was 24 cm^3/h and analyses were performed essentially as described in ref. [10] (cf. ref. [9]). Equilibration of the column was checked as in Ref. [10]. After equilibration, a sample of native PRA:IGPS was applied to the Sephacryl S-300 HR column, by which means the enzyme was rapidly converted into an SDS–polypeptide complex. The protein

concentration was determined as described before [10].

Binding studies [11,12] employing both gel filtration [9] and ultrafiltration showed that the protein is practically saturated with DS at 1.6 mM SDS, i.e. just below its CMC (1.8 mM SDS) in 0.05 M sodium phosphate, pH 6.9, 1 mM EDTA, 0.2 mM DTE, and 3 mM NaN_3, above the critical micelle temperature (25°C, ref. [13]).

2.3. Neutron scattering

The neutron camera was the D11 instrument at the High-Flux Reactor of the Institut Laue-Langevin, Grenoble [14]. The wavelength used was 1.0 nm; the sample-to-detector distances were 1.1 and 5.5 m. The sample solutions were contained in quartz cells of 1.00 mm optical pathlength (HELLMA, Müllheim, Germany); the irradiated volume was 200 mm^3.

The temperature of the samples was kept at 24 to 25°C, that is, above the critical micelle temperature [13].

The incoherent, hence isotropic, scattering of a (light) water sample of 1.00 mm thickness was used for calibrating the product of the neutron intensity I_0 in the primary beam and the solid angle $\Delta\Omega$ subtended by the detection elements [15]. The known M_r of the whole protein and of its fragments, and the concentrations c of polypeptide, as determined by total amino acid analyses, allowed us to calculate the number densities $n = cN_A M_r$ of the particles. After subtraction of the Q-independent (i.e. isotropic) incoherent scattering we determined the coherent differential scattering cross sections per unit solid angle and per particle (short: cross section), $d\sigma(Q)/d\Omega = I_s(Q)/(I_0 \Delta\Omega T n d)$, with $I_s(Q)$, the intensity scattered by the sample; T, the attenuation of the primary beam; and d, the thickness of the sample.

All data were measured at a protein concentration of 2 mg/cm^3. Due to long-range repulsive forces between the particles, the deviation from a random spatial distribution of the particles within the sample volume becomes tangible even at these low concentrations. The resulting interparticle interference effect diminishes the intensity scattered at very low angles by a few percent. We corrected for this effect by using the extrapolated particle structure factor (at small Q) which had been obtained from our previous experiments [7].

3. Results and discussion

Our data points, Fig. 1, show the particle cross sections at an ^2H_2O concentration of 95%. The different curves refer to the various subsaturating concentrations of free SDS, i.e. 1.6, 1.4, 1.2, 1.0, 0.8, and 0.6 mM. The continuous lines represent fits of the data points to a series of Fourier-transformed spline functions [16]. Corresponding data sets for the same SDS concentrations were also obtained at ^2H_2O concentrations of 85, 44, and 0% (data not shown).

The coherent part of the secondary waves scattered by the ensemble of atomic nuclei contained in the sam-

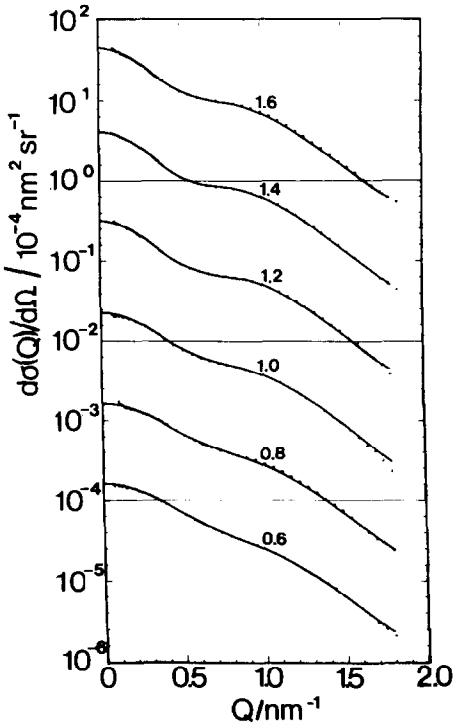

Fig. 1. Neutron small-angle scattering from SDS–protein complexes with PRA-isomerase:IGP-synthase (M_r = 49 484) at various free SDS concentrations in 95% ^2H_2O. $d\sigma(Q)/d\Omega$ is the coherent scattering cross section per unit solid angle per particle; $Q = (4\pi/\lambda)\sin(\Theta/2)$ is the momentum transfer; λ is the neutron wavelength; and Θ is the full scattering angle. The data were obtained with 2 mg protein per cm^3. The free SDS concentrations are given in mM units at each curve: 1.6 mM (top; ordinate scale 1:1), 1.4 mM (ordinate scale 1:10), 1.2 mM (ordinate scale 1:100), 1.0 mM (ordinate scale 1:1000), 0.8 mM (ordinate scale 1:10000), and 0.6 mM (ordinate scale 1:100000). The solid line is the fit of Fourier-transformed spline functions to the data. The statistical deviation of the data points is less than the thickness of the solid line. Similar data sets have been obtained for 84, 44, and 0% ^2H_2O (data not shown).

ple are completely described by their amplitudes and their phases. From the total of the coherent *amplitudes* only that part contributes to the observable intensity which is *in excess* of the mean of the coherent scattering amplitudes of the buffer molecules contained in the equal volume as occupied by the particle. The sum of the coherent excess amplitudes of all the secondary waves originating from the nuclei of a single particle is called the (coherent) excess particle amplitude (in short, excess amplitude).

The *phases* of all the secondary waves which are scattered into the forward direction, $Q \rightarrow 0$, are identical (with the exception of the secondary waves that are scattered by the protons, which are shifted, with respect to the secondary waves scattered by the other nuclei, by the constant phase angle π). The excess amplitude can therefore be determined uniquely as the square root of the experimentally observed cross section extrapolated to their value at $Q = 0$. It is one of the great advantages of neutron scattering that the accuracy of this measurement is better than some few percent.

In Fig. 2, these square roots (hence the excess amplitudes) are plotted vs. the relative ^2H_2O concentration (bottom scale) and the scattering amplitude density (top scale) of the buffer. Each straight line represents, at different contrasts, the results of the measurements at a constant free SDS concentration. Note that at 0.6 mM free SDS concentration, fewer SDS molecules are bound than at 1.6 mM. This explains the higher value of $(d\sigma(Q \rightarrow 0)/d\Omega)^{1/2}$ in the ^2H_2O samples for 1.6 mM free SDS concentration.

The slope of the lines (excess particle amplitude vs. buffer amplitude density) is the 'invariant volume' [17] occupied by one particle, i.e. the volume that is inaccessible to the protons and/or deuterons of the buffer (this volume excludes the volume occupied by bound water molecules and half of the mean volume of a water molecule per each exchangeable proton [18]).

The total invariant volume consists of the partial volumes of the polypeptide chain plus the volume of one SDS molecule multiplied with their number. In other words, the difference between the invariant volume of the SDS–protein complex and the invariant volume of the polypeptide chain (the latter is known to be 45–50 nm^3, the slope of the dashed line in Fig. 2) is due to the additional volume conferred by the bound DS molecules. Using the known volume 0.410 nm^3 of one single SDS molecule [8], we can calculate

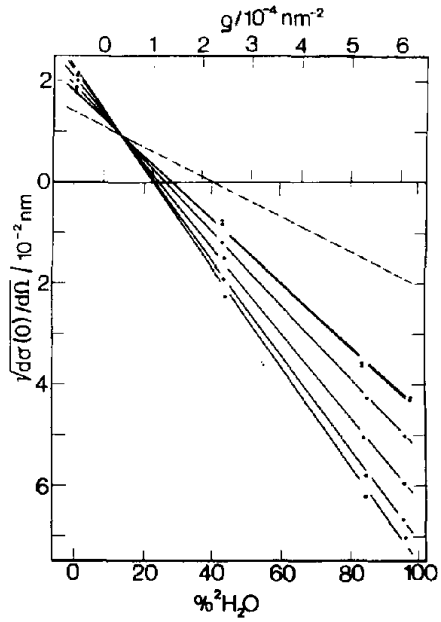

Fig. 2. Square root of zero angle scattering $(d\sigma(0)/d\Omega)^{1/2}$ (i.e. the excess amplitude) per particle versus ^2H_2O concentration (bottom abscissa line; the corresponding scattering amplitude density of the buffer is shown at the top abscissa line). The slope of the lines is the 'invariant volume' of the particle which is inaccessible to the hydrogen atoms of the buffer. Dashed line: protein alone. The steepest line is that obtained with the saturated complexes in buffer containing 1.6 mM SDS, i.e. slightly below the CMC. The other lines (with decreasing slope) are those obtained with the subsaturating SDS concentrations indicated in the legend to Fig. 1 in the same order.

the number of bound DS molecules, Table 1. Since the scattering amplitude density of SDS molecules is 0.389×10^{-4} nm^{-2} [8], which corresponds to 14% ^2H_2O, the solid lines in Fig. 2 cross the dashed line at this abscissa value.

The forward scattering data confirm the approximate stoichiometry, at saturation, of one SDS molecule bound per two amino acid residues. At reduced, subsaturating, concentrations of free SDS in equilibrium with the bound DS, the 1:2 stoichiometry between the number of DS molecules and the number of amino acid residues steadily decreases to a 1:4 stoichiometry at 0.5 CMC.

The neutron data, as taken from Table 1, are shown in Fig. 3 together with the binding curves obtained by gel chromatography of the protein with ^{35}S-SDS [10]. The binding has also been determined by the Methylene Blue method [12] with samples corresponding to those used for neutron scattering experiments, but the accu-

Table 1
Structural consequences of the diminution of the free SDS concentration to subsaturating levels

Free SDS concentration in the buffer		A	B/nm	C/nm	D/nm
(mM)	%CMC				
1.6	89	235 ± 6	7.5	13	
1.4	78	214	7.4	13	
1.2	66	183	7.1	13	
1.0	56	135	6.9 (shoulder at 9)	12	
0.8	44	105			6.6 (shoulder at 9)
0.6	33	100 ± 3			6.2

The number of SDS molecules bound to the water-soluble enzyme PRA-isomerase:IGP-synthase (M_r = 49 484) per (N + M + C)-particle (see Fig. 5) is indicated in column A. For the *three-micelle complex*, the mean distance between the two neighbouring micelles N and M, superimposed on the mean distance between the two neighbouring micelles M and C is indicated in column B; and the distance between the two external micelles N and C is indicated in column C. For the *two-micelle complex*, the distance between the two neighbouring micelles NM and C is indicated in column D. The number of amino acid residues in the micelles N, M, and C is about 87, 193, and 160, respectively. Upon diminution of the free SDS concentration in the buffer the number of residual SDS molecules within each micelle remains proportional to the number of amino acid residues.

racy is not better than ± 10%. The difference in the binding observed with neutron scattering and with gel filtration may possibly be attributed to the effect of heavy water on the stability of hydrogen bonds. SDS binding to the protein upon gel filtration may also have become enhanced by interaction of the SDS–protein complex with SDS bound to the gel matrix. This may have happened when samples were prepared for neutron scattering experiments and when binding was determined by use of radioactive tracer. Before the neutron scattering measurements, the samples were finally dialyzed, which could have lowered the binding to the level corresponding to the concentration of free SDS monomers. The SDS binding would be sensitive to this hypothetical effect at SDS concentrations below saturating levels.

The cross sections extrapolated to zero momentum transfer are easily determined directly from the scattering curves. At larger momentum transfers, however, the curves are quite featureless and difficult to assess. This is due to the superposition, in the scattering space, of the terms that arise from different, but possibly nevertheless well defined, structural features in real space. In certain cases, as in the present one, these structural details may show up much more clearly in the Fourier transforms of the scattering patterns. In small-angle scattering, they represent the orientational averages of the convoluted structure in real space, i.e. the pair distance distribution functions (PDDFs) [16]. The

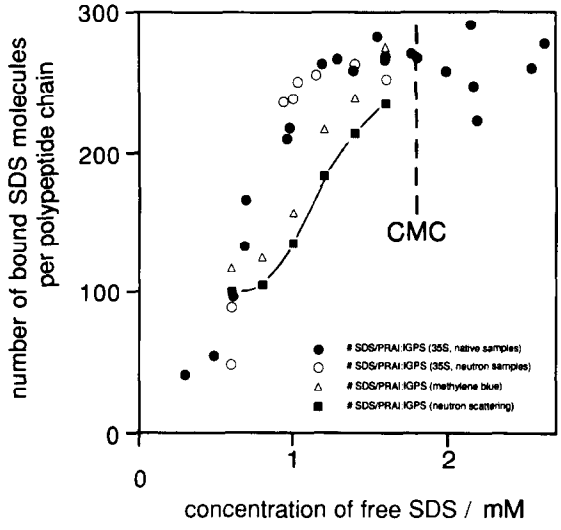

Fig. 3. Stoichiometry of SDS binding per polypeptide chain vs. equilibrium free SDS concentration at subsaturating values: ■, neutron scattering data from Table 1 (the nominal SDS concentrations may be too high by ~0.1 mM, the data points are connected by an eye-guiding line); ●, binding with native samples determined by gel filtration in the presence of ^{35}S-SDS; ○, binding after reequilibration of samples corresponding to those used used for neutron scattering with ^{35}S-SDS on Sephacryl S-300 HR; △, binding determined by the Methylene Blue method [12] with samples corresponding to those used for neutron scattering experiments. For the points indicated by the full symbols the accuracy of the free SDS concentration is 3% and that of the binding values is about ± 5% [10]. The accuracy of the Methylene Blue values is not better than ± 10%.

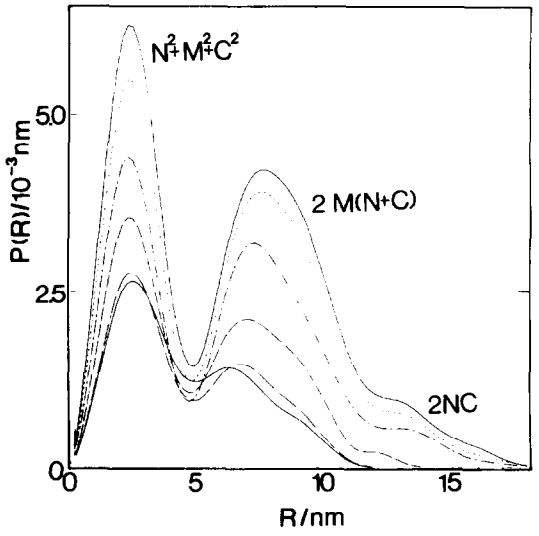

Fig. 4. Pair–distance distribution functions for the different concentrations of free SDS in the 95% ^2H_2O buffer. The curves were calculated from the data points in Fig. 1 with the same order of SDS concentrations from top to bottom. See the text for interpretation of distances and areas.

PDDFs describe the probability of finding a given distance between any two volume elements within the particle, weighted with their excess amplitude densities (Fig. 4). 4π times the areas under the respective curves are the cross sections at zero angle (i.e. the squares of the excess amplitudes [16]).

One of the important results of our previous study [7] is the proof that the saturated complex consists of three widely separated protein-decorated micelles. This finding allows us to discuss the PDDFs, as already exemplified in our previous study, as being due to the *spatial distribution of the excess amplitude* $(M+N+C)$ over the three micellar substructures M and N and C. The six terms of the corresponding *cross section* $(M+N+C)^2 = M^2+N^2+C^2+2MN+2MC+2NC$ and the six PDDFs related to them can be sorted, according to the distances involved, within three groups:

(1) The small distance peak in the PDDFs shown in Fig. 4, which is marked by $N^2+M^2+C^2$, is the sum of the single PDDFs of the three individual micelles. 4π times the area under this peak is the sum of the squared excess amplitudes of the three individual micelles. We call this peak, which extends up to 4.5 nm, the 'self-term' peak.

(2) The most probable distance between two neighbouring micelles is 7.5 nm, as given by the intermediate distance position of the 'interference term' peak marked $2M(N+C)$. This peak is due to scattering interference between pairs of micelles, one micelle being the middle micelle, and the other micelle one of the terminal micelles. 4π times the area under this peak is the sum $(2MN+2MC)$ of twice the product of the excess amplitude of the micelle M and that of the micelle N; plus twice the product of the excess amplitude of the micelle M and that of the micelle C. Near saturation of the complex, this peak extends from 4.5 to about 12 nm. With diminishing number of SDS molecules in the complex, the maximum of the first interference peak is continously shifted from 7.5 to 6.2 nm, which indicates a diminution of the mean distance between the middle micelle and each of the two external micelles.

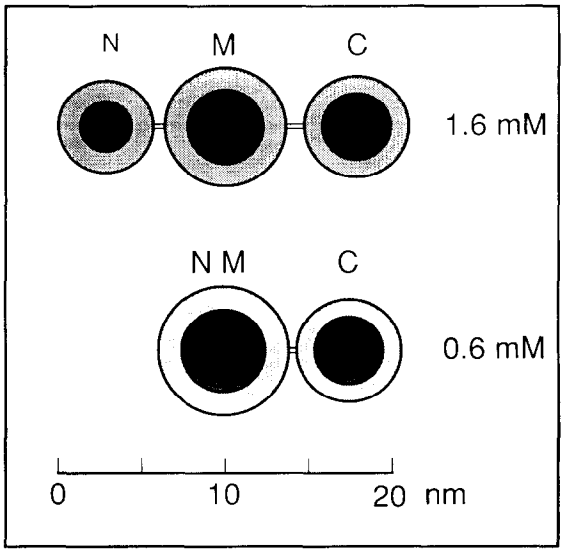

Fig. 5. Schematic scale models of the mutual disposition of the three protein-decorated micelles in buffer containing 1.6 mM SDS (0.9 CMC, top) and of the two protein-decorated micelles in buffer containing 0.6 mM SDS (0.3 CMC, bottom). The independent micelles N (N-terminal), M (middle) and C (C-terminal) of the three-micelle complex are connected, at saturation, by flexible oligopeptide linkers about 5 or 6 amino acid residues long; with decreasing SDS concentration to subsaturating levels, the small micelle N coalesces with micelle M; and micelle C approaches micelle M. The difference in contrast between the dodecyl chain cores and the surrounding protein sulfate shell is visualized by a different shading. This information was determined in a previous experiment [7]; the internal structure is *not* the subject of this present paper.

(3) The PDDFs at high SDS concentrations show a shoulder at 14.5 nm, marked 2NC. This shoulder is due to a large distance 'interference term' peak. The interference has its origin from one single pair of micelles, both situated at the terminal positions: the amino-terminal micelle N, and the carboxyl-terminal micelle C. 4π times the area under this peak is twice the product of the excess amplitudes of these two micelles. With diminishing number of SDS molecules in the complex, this third peak disappears completely: the three-micelle complex has become a two-micelle complex. From the ratio of the self-term to the single remaining interference term we conclude that upon diminishing the SDS concentration to very low subsaturating values the small N-terminal micelle N coalesces with the middle micelle M (Fig. 5). The relative molecular mass of the protein moiety is the same for both the two- and three-micelle complexes, since the M and N micelles are combined in the two-micelle complex.

4. Conclusion

We have shown [7] that the polypeptide chain stabilizes the micelles; otherwise saturation would not be achieved below the CMC [2,3]. Such stabilization is also observed when SDS binds to poly(oxyethylene) [8]. *Our present data prove that the stabilisation is effective even at drastically reduced* SDS *concentrations, far below the* CMC.

The secondary structure of the native protein consists of alternating amphiphilic α-helices (a total of 17) and β-strands (a total of 16) interconnected by 32 surface loops [6]. The three-micellar configuration at 1.6 mM defines two oligopeptide linkers. At saturation, each intermicellar linker is situated in both domains between the section of the polypeptide chain which forms, in the native enzyme, the second β-strand and that which forms the second α-helix [7]. Upon lowering the SDS concentration, the first intermicellar linker in the N-terminal IGPS domain disappears; that in the C-terminal PRAI domain, however, persists irreversibly. This is consistent with the measurement of the elution volume of the complex which shows a steep increase on lowering the SDS concentration from 1.6 down to about 1.0 mM. Below this value the increase is less pronounced (Fig. 4 in ref. [9]). On increasing the SDS concentration from 0 up to about 0.4 mM, the elution volume of the complex shows a first steep decrease (Fig. 1 in Ref. [7]). The structural basis of these observation is the formation, depending on the number of bound SDS molecules, of either a two-micelle complex or a three-micelle complex.

Acknowledgements

The work was supported by the Swedish Natural Science Research Council; the O.E. and Edla Johansson Science Foundation; the Swedish National Board for Technical Development, Grant No. 89-519P (PL, MS, EM). We thank Kasper Kirschner and Halina Szadkowski, Biozentrum Basel, for the preparation of the enzyme and for many valuable suggestions and comments.

References

[1] J.A. Reynolds and C. Tanford, J. Biol. Chem. 245 (1970) 5161.
[2] K. Shirahama, K. Tsujii and T. Takagi, J.Biochem. (Tokyo) 75 (1974) 309.
[3] T. Takagi, K. Tsujii and K. Shirahama, J. Biochem. (Tokyo) 77 (1975) 939.
[4] W.L. Mattice, J.M. Riser and D.S. Clark, Biochemistry 15 (1976) 4264; A.J.H. Damon and G.C. Kresheck, Biopolymers 21 (1982) 895.
[5] P. Lundahl, E. Greijer, M. Sandberg, S. Cardell and K.-O. Eriksson, Biochim. Biophys. Acta 873 (1986) 20.
[6] J.P. Priestle, M.G. Grütter, J.L. White, M.G. Vincent, M. Kania, E. Wilson, T.S. Jardetzky, K. Kirschner and J. Jansonius, Proc. Natl. Acad. Sci. USA 84 (1987) 5690.
[7] K. Ibel, R.P. May, K. Kirschner, H. Szadkowski, E. Mascher and P. Lundahl, Eur. J. Biochem. 190 (1990) 311.
[8] B. Cabane and R. Duplessix, J. Phys. (Paris) 43 (1982) 1529; B. Cabane and R. Duplessix, J. Phys. (Paris) 48 (1987) 651; B. Cabane, R. Duplessix and T. Zemb, J. Phys. (Paris) 46 (1985) 2161.
[9] E. Mascher and P. Lundahl, J. Chromatogr. 476 (1989) 147.
[10] M. Wallstén and P. Lundahl, J. Chromatogr. 512 (1990) 3.
[11] T. Takagi, J. Miyake and T. Nashima, Biochim. Biophys. Acta 626 (1980) 5.
[12] K. Hayashi, Anal. Biochem. 67 (1975) 503.
[13] R. Becker, A. Helenius and K. Simons, Biochemistry 14 (1975) 1835.
[14] K. Ibel, J. Appl. Crystallogr. 9 (1976) 269; P. Lindner, R.P. May and P.A. Timmins, Physica B 180/181 (1992) 967.
[15] R.P. May, K. Ibel and J. Haas, J. Appl. Crystallogr. 15 (1982) 15.
[16] O. Glatter, J. Appl. Crystallogr. 10 (1977) 415.
[17] V. Luzzati, A. Tardieu and L.A. Aggerbeck, J. Mol. Biol. 131 (1979) 435.
[18] G.G. Kneale, J.P. Baldwin and E.M. Bradbury, Q. Rev. Biophys. 10 (1977) 485.